ORIGINAL PAPER

Preparation and characterization of lithium ion conducting ionic liquid-based biodegradable corn starch polymer electrolytes

Chiam-Wen Liew · S. Ramesh · K. Ramesh · A. K. Arof

Abstract Thin films of biodegradable corn starch-based biopolymer electrolytes were prepared by solution casting technique. Lithium hexafluorophosphate (LiPF$_6$) and 1-butyl-3-methylimidazolium trifluoromethanesulfonate (BmImTf) were employed as lithium salt and ionic liquid, respectively. With reference to the temperature dependence study, Arrhenius relationship was observed. The highest ionic conductivity of $(6.00 \pm 0.01) \times 10^{-4}$ S cm^{-1} was obtained at 80 °C. Based on x-ray diffraction (XRD) result, the peaks became broader with doping of ionic liquid revealing the higher amorphous region of the biopolymer electrolytes. Ionic liquid-based biopolymer electrolytes exhibited lower glass transition temperature (T_g).

Keywords Corn starch · BmImTf · XRD · DSC

Introduction

From a green viewpoint, many researchers have a keen interest on ionic liquid-based biopolymer electrolytes. Ionic liquid-based polymer electrolytes have a great tendency to replace conventional polymer electrolytes in electrochemical, electronic and power storage devices as ionic liquid provides potential environmental advantages relative to conventional solvents. Room temperature ionic liquids (RTILs) are molten organic salt consisting of bulky organic cations with delocalized charges and organic or inorganic anions [1]. RTILs are promising candidates because of their inherent physical and chemical characteristics such as nonvolatility, nonflammability, negligible vapor pressure, low melting point, low toxicity, high conductivity and excellent thermal and electrochemical stabilities as well as a wide electrochemical window [1–3].

In order to develop environmentally friendly polymer electrolytes, biodegradable polymer has been widely investigated to alternate conventional nondegradable or incompletely degrading synthetic biopolymers. Starch is an abundant, renewable and biodegradable raw material with low price [4]. Other unique properties are excellent thermal and steel adhesion properties, superior biocompatibility, good solubility, high recrystallization stability of the amorphous phase and great ability to form films [5–7]. In this present work, lithium hexafluorophosphate (LiPF$_6$) was chosen because of its good environmental impacts, high solubility and high conductivity in various solvents [8]. It possesses many advantages, for example, excellent electrical stability, low moisture absorption and is less dangerous and poisonous [9, 10]. In addition, it could form suitable solid electrolyte interface (SEI) membrane in electrodes, especially in cathode. It also implements the passivation for anode current collectors to prevent their dissolution [9]. Ionic liquid, 1-butyl-3-methylimidazolium trifluoromethanesulfonate (BmImTf) were embedded in this work. This ionic liquid consists of 1-butyl-3-methylimidazolium cation (BmIm$^+$) and trifluoromethanesulfonate (or known as triflate) anion (Tf$^-$). Among all the cations, 1,3-dialkylimidazolium (Im) is the appealing cation because of its favorable properties and ease to gather abundant and useful information [11]. Other than that, the imidazolium ILs bearing hydrophilic anions are capable of dissolving corn starch [12]. On the other hand, triflate anion was selected due to its bulky structure. This bulky anion favors the delocalization of

C.-W. Liew · S. Ramesh (✉) · K. Ramesh · A. K. Arof
Centre for Ionics University Malaya, Department of Physics,
Faculty of Science, University of Malaya,
Lembah Pantai,
50603, Kuala Lumpur, Malaysia
e-mail: rameshtsubra@gmail.com

C.-W. Liew
e-mail: liewchiamwen85@gmail.com

charge and reduces the interaction between anion and cation in the complex with lower lattice energy, leading to the high degree of dissociation [13].

Experimental

Materials

Ionic liquid-based biopolymer electrolytes were prepared by solution casting technique. Biodegradable corn starch (Sigma-Aldrich), lithium hexafluorophosphate (LiPF$_6$) (Aldrich) and 1-butyl-3-methylimidazolium trifluoromethanesulfonate (BmImTf) (Aldrich) were employed as host polymer, lithium salt and ionic liquid, respectively.

Preparation of thin films

Different stoichiometric quantities of BmImTf were doped in the solution with a fixed ratio of 80 wt.% of corn starch to 20 wt.% of LiPF$_6$. The quantity of materials added is expressed as weight percent (wt.%) and the designation of the samples are as tabulated in Table 1. Appropriate amounts of corn starch, LiPF$_6$ and BmImTf were dissolved in distilled water. The solution was then stirred overnight at 80 °C. The resulting solution was thus cast on a glass Petri dish and dried in oven, forming biopolymer films.

Characterizations

All the samples were subjected to ac-impedance spectroscopy, x-ray diffraction (XRD), scanning electron microscopy (SEM) and differential scanning calorimetry (DSC).

Temperature dependence–ionic conductivity studies

The prepared samples were subjected to ac-impedance spectroscopy. The thickness of the samples was measured by

Table 1 The nomenclature of samples with different stoichiometric amounts of materials added into polymer electrolytes and its activation energy

Corn starch–LiPF$_6$ (wt.%)	BmITf (wt.%)	Designations	Activation energy, E_a (eV)
100	–	Tf 0	0.13
80	20	Tf 2	0.12
70	30	Tf 3	0.11
50	50	Tf 5	0.10
30	70	Tf 7	0.02
20	80	Tf 8	0.01
10	90	Tf 9	0.02

using a micrometer screw gauge. The ionic conductivities of the samples were determined by using HIOKI 3532-50 LCR HiTESTER over a frequency range between 50 Hz and 5 MHz. The ionic conductivity was measured from ambient temperature to 80 °C. Samples were mounted on the holder with stainless steel (SS) blocking electrodes under spring pressure with the configuration SS/SPE/SS. The bulk ionic conductivity is determined by using the equation below.

$$\sigma = \frac{l}{R_b A} \qquad (1)$$

where l is the thickness (cm), R_b is bulk resistance (Ω) and A is the known surface area (cm^2) of polymer electrolyte film. The semicircle fitting was accomplished to obtain R_b value. As shown in Fig. 1, R_b of the thin electrolyte films is calculated from interception of the semicircle and the spike.

X-ray diffraction (XRD) studies

The amorphous nature of biopolymer electrolytes was investigated via XRD study. The XRD patterns were recorded on a Siemens D 5000 diffractometer with Cu-Kα radiation (λ=1.54060 Å) over the range of 2θ=5–80° at ambient temperature.

Differential scanning calorimetry (DSC)

DSC analysis was evaluated under nitrogen flow rate of 10 ml min^{-1} by the means of TA Instrument Universal Analyzer 2000 which comprised of DSC Standard Cell FC as the main unit and Universal V4.7A software. Samples weighing 4–5 mg hermetically sealed in the aluminum T
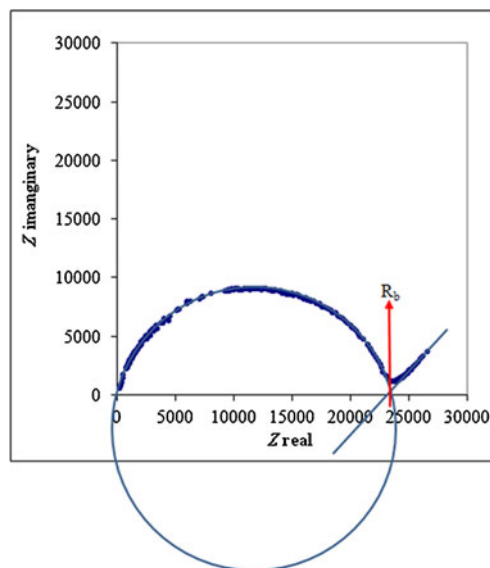

Fig. 1 Typical Cole–Cole plot of complex impedance of Tf 0 at room temperature

zero pans and an empty hermetically sealed aluminum pan was used as the reference cell. As a preliminary step, the samples were heated from 25 °C to 105 °C to remove any trace amount of solvent and water at a heating rate of 30 °C min^{-1} and were maintained at 105 °C for 5 min to ensure complete evaporation. Subsequently, the samples were rapidly cooled to −40 °C and reheated to 70 °C at the preset heating rate. The final heating scan was used to evaluate T_g.

Results and discussion

Ac–impedance studies

A typical Cole–Cole plot of complex impedance of Tf 0 is depicted in Fig. 1. As can been seen, the complex impedance plot is composed of two well-defined regions: a slanted spike at low frequency and a semicircle at high frequency. The semicircle represents the combination of bulk resistance and bulk capacitance of polymer matrix in parallel arrangement. The resistance reveals the ionic transportation through the voids within the polymer matrix which can be detected by a resistor. On the other hand, the capacitance implies the polarization of immobile polymer chain in the alternating field which is represented by the capacitor. A slanted spike is observed instead of a vertical spike. This discloses the nonideal mode of capacitance behavior in the polymer electrolytes and ultimately leads to the formation of electrical double layer at the electrode–electrolyte boundary as a result of the polarization effect when the electrical potential alternates between the positive and negative electrodes in the alternate current field. The configuration of this constant phase element (CPE) further entails non-Debye properties of the polymer electrolytes. On the other hand, the degree and slope of the inclination of the peak corresponds to the relaxation time distribution where the charge carriers are accumulated at the electrode–electrolyte interface before the electric field changes the direction.

However, upon inclusion of ionic liquid, the semicircle becomes incomplete as illustrated in Figs. 2 and 3. It suggests that the plasticizing effect of ionic liquid weakens the interactive coordination bonds within the polymer system. Hence, it reduces the polarization of the dipole in the polymer chain and hinders the charge accumulation at the electrode–electrolyte interface, giving rise to the imperfection of capacitance behavior. The semicircle disappears with impregnation of 80 wt.% of BmImTf. It is due to the random dipole orientation in the side chains of the polymer matrix and induction to the noncapacitance properties of the polymer electrolytes. Therefore, only the resistive components in the polymer electrolytes prevail at this moment and, thus,
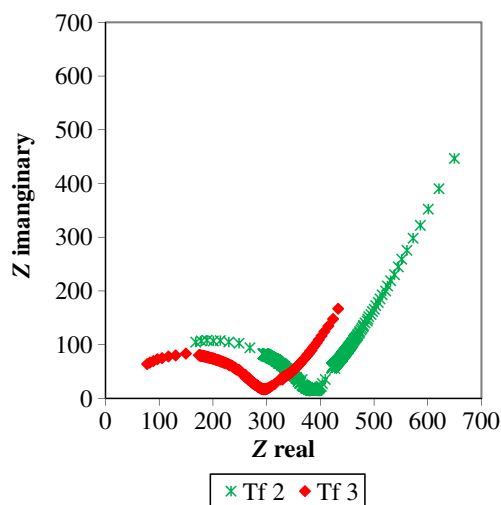

Fig. 2 Typical Cole–Cole plots of complex impedance of Tf 2 and Tf 3 at room temperature

construct a local effective conducting pathway for ionic conduction mechanism. As a result, it promotes the ionic migration. It can be concluded that current charge carriers are ions which responsible for the ionic transportation with the disappearance of the semicircle region.

Another observation is also obtained from Figs. 1, 2 and 3. The R_b values decrease with BmImTf mass loadings. In other words, the ionic conductivity increases with BmImTf concentration. It is mainly attributed to the strong plasticizing effect of ionic liquid. The plasticizing effect would soften the polymer backbone, improve the flexibility of polymer matrix and then promote the ion dissociation from the transient coordinative bonds. As a result, it initiates the ionic migration within the polymer matrix and yields the ionic conduction, resulting in higher ionic conductivity.
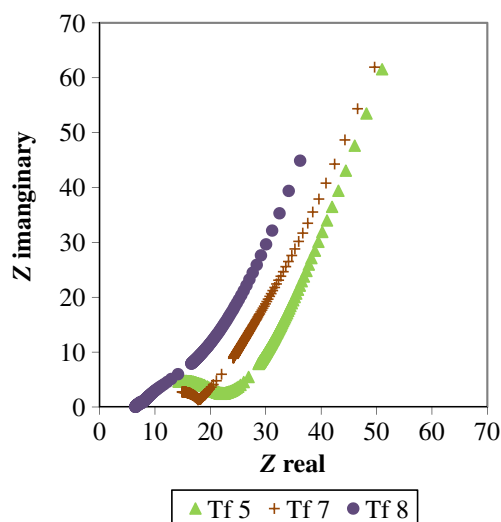

Fig. 3 Typical Cole–Cole plots of complex impedance of Tf 5, Tf 7 and Tf 8 at room temperature

Temperature dependence–ionic conductivity studies

Figure 4 portrays temperature dependence–ionic conductivity of Tf 0, Tf 2, Tf 3, Tf 5, Tf 7, Tf 8 and Tf 9 from ambient temperature to 80 °C. There is no abrupt change in the value of conductivity with respect to temperature, inferring no phase transitions within the temperature regime for all the complexes [14]. As can been seen, the ionic conductivity increases with temperature. High internal vibrational mode of polymer complex is produced as temperature increases. This high kinetic energy of molecules in the polymer membrane would improve the bond rotation and help in destroying the weak interactive bonds between the oxygen atom of corn starch and lithium cations (Li$^+$). Thus, the ions are more easily to be decoupled from the polymer backbone which assists the ionic migration within the polymer matrix and increases the ionic conductivity at a high temperature. As determined in Fig. 1, the increase of ionic conductivity is in this order: Tf 0 < Tf 2 < Tf 3 < Tf 5 < Tf 7 < Tf 9 < Tf 8. This is in good agreement with the previous study. Tf 8 achieves the highest ionic conductivity of $(6.00 \pm 0.01) \times 10^{-4}$ S cm^{-1} at 80 °C. However, the ionic conductivity is decreased by adding 10 wt.% more of BmImTf (or denoted as Tf 9). It is suggestive of the ion association which leads to the formation of ion pairs and ion aggregates. Eventually, it impedes the ionic transportation within polymer matrix by blocking the conducting pathway.

As shown in Fig. 1, the regression values of all the samples are close to unity. Thus, it declares that the samples follow the Arrhenius behavior and further implies the ionic hopping mechanism within the polymer complexes. In this thermally activated phenomenon, the conductivity is expressed as follow:

$$\sigma = A \exp\left(-\frac{E_a}{kT}\right) \qquad (2)$$

where A is a constant which is proportional to the amount of charge carriers, E_a is activation energy, k is Boltzmann constant and T is the absolute temperature in Kelvin. As aforementioned, the charge carriers are dissociated from corn starch polymer backbone. Arrhenius theory states that this ionic decoupling would create the vacancy or voids in the polymer electrolytes. So, the neighboring ions from adjacent sites will occupy the vacant site, recoordinate with the polymer chain and, eventually, generate the ionic hopping process. It can be concluded that more vacancies and ionic transportation are formed as the charge carriers are more easily detached from the polymer chain at an elevated temperature.

In order to probe the ion dynamic of polymer electrolytes further, activation energy, E_a is determined by fitting it in the Arrhenius equation. E_a is defined as the required energy to overcome the reorganization and reformation of the interactive bonds between polymer chain and Li$^+$ [14, 15]. As shown in Eq. 1, E_a is inversely proportional to ionic conductivity. The E_a values are tabulated in Table 1. Among the samples studied, the most ionic conducting sample, Tf 8, illustrates the lowest E_a value which indicates that ionic conduction is the most favorable. The E_a value is greatly decreased with increasing BmImTf mass fraction. It is primarily related to the plasticizing effect of the ionic liquid with predominant amorphous region. Less energy is required to break the physical and chemical bonds as the ionic liquid assists in weakening the interaction within the polymer chains. On comparison between Tf 2, Tf 3, Tf 5, Tf 7 and Tf 8, Tf 8 shows the lowest E_a values because of its strong plasticizing effect. This would weaken the coordinative bonds and, therefore, it requires lesser energy to disrupt the linkages of polymer chains. Theoretically, Tf 9 should display lower activation energy due to the plasticizing effect of ionic liquid. However, an opposite result has been observed. Again, it reveals the formation of ion pairs and ion aggregates which acquires more energy to break the interactive bonds between the ion pairs and ion aggregates with a restricted polymer segmental mobility.

Fig. 4 Arrhenius plot of ionic liquid-free and ionic liquid-based biopolymer electrolytes
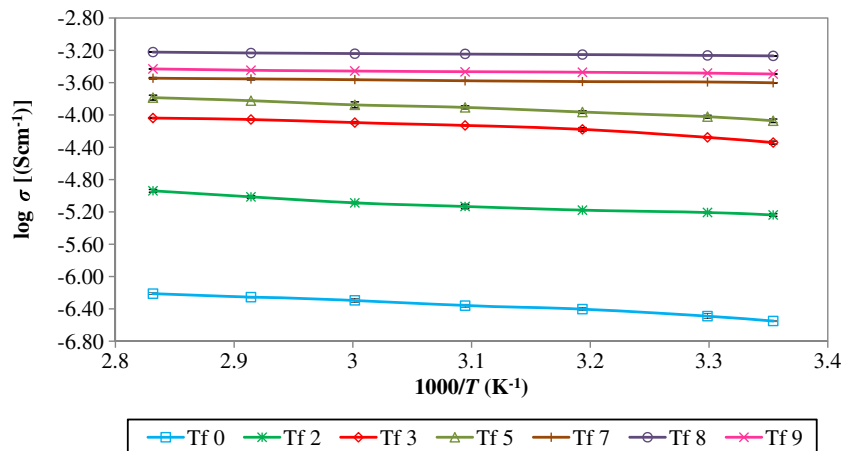
X-ray diffraction XRD studies

Figure 5 exemplifies the XRD patterns of pure corn starch, pure $LiPF_6$ and Tf 0, whereas Fig. 6 demonstrates the x-ray diffractograms of Tf 0, Tf 3, Tf 5 and Tf 8. As shown in Fig. 5b, the sharp intense peaks at $2\theta=8°$, 21.7°, 25.3°, 28.3°, 35.3°, 37°, 42.8°, 49.3°, 55.9°, 60.6°, 61° and 68.4° disclose the crystalline character of $LiPF_6$. On the contrary, pure corn starch shows a broad peak at 16° and a medium sharp peak at 23.3° and further divulges its semicrystalline behavior. Upon inclusion of lithium salt, these diffraction peaks have been shifted to 17° and 22.2°, asserting the change in crystallographic organization [15]. These peaks become broader compared to neat pure corn starch. The relative intensity of the peaks also decreases significantly by doping lithium salt. This signifies that the addition of lithium salt disorders the ordered arrangement within the polymer membrane and reduces the crystallinity degree. All the crystalline peaks of $LiPF_6$ are absent in TF 0. This signifies that $LiPF_6$ is well dissociated to form the complexation between corn starch and $LiPF_6$ [16].

The crystalline peaks are noted to disappear in ionic liquid-based biopolymer electrolytes. This implies the complete dissolution of $LiPF_6$ in the polymer electrolytes and contributes to the complexation of $LiPF_6$ with corn starch and BmImTf [17]. Upon addition of 30 wt.% of BmImTf, the two diffraction peaks of corn starch are still present. As can be observed, these two characteristic peaks have been shifted to 2θ angles of 15.4° and 24.3°. However, the peaks become broader in comparison with Tf 0. The intensity of a peak is also drastically reduced with inclusion of 30 wt.% of BmImTf. It can be inferred that addition of ionic liquid would weaken the transient bonds within the polymer system, distort the ordered arrangement of the polymer backbone and eventually decrease the degree of crystallinity. In other words, it increases the amorphous region in polymer electrolytes, facilitates the ion mobility and provides a more flexible backbone, which in turn leads to higher ionic conductivity. The amorphous behavior becomes more visible with increasing the ionic liquid loadings. Obviously, the XRD pattern has undergone the change in shape, from two weak peaks to a broad band. Tf 5 is illustrated to show a more intense band than Tf 8 by comparing Fig. 3c with d. This reveals that Tf 5 has lesser amorphous degree which leads to lower ionic conductivity. As shown in Fig. 6, Tf 8 illustrates the lowest peak intensity and indicates the highest amorphous degree in comparison with other samples studied. This highest amorphous behavior of Tf 8 would enhance the ion transportation to a greater extent and thereby increase the ionic conductivity to a maximum.

Differential scanning calorimetry (DSC)

The thermal properties of samples are examined through DSC analysis. The result is shown in Fig. 7. A small decrease in heat, from exothermic to endothermic, is known as glass transition temperature (T_g). A T_g is defined as a critical temperature at which the amorphous material changes its behavior from glassy state to rubbery state. Pure corn starch demonstrates T_g of 56 °C. However, T_g exhibits an abrupt decrease upon addition of $LiPF_6$ and a subambient T_g of −19 °C is observed. The decrease in T_g infers the higher segmental mobility of polymer backbone. This is due to the distortion of the weak interactive hydrogen bonds within the polymer chains by doping lithium salt which eventually forms the complexation. The relative T_g value is further decreased with addition of ionic liquid. Strong plasticizing effect is the main attributor for this phenomenon. Ionic liquid weakens the dipole–dipole interactions and transient inter- and intramolecular bonds among starch granules. Thus, it tends to soften the polymer network and improves the flexibility of polymer

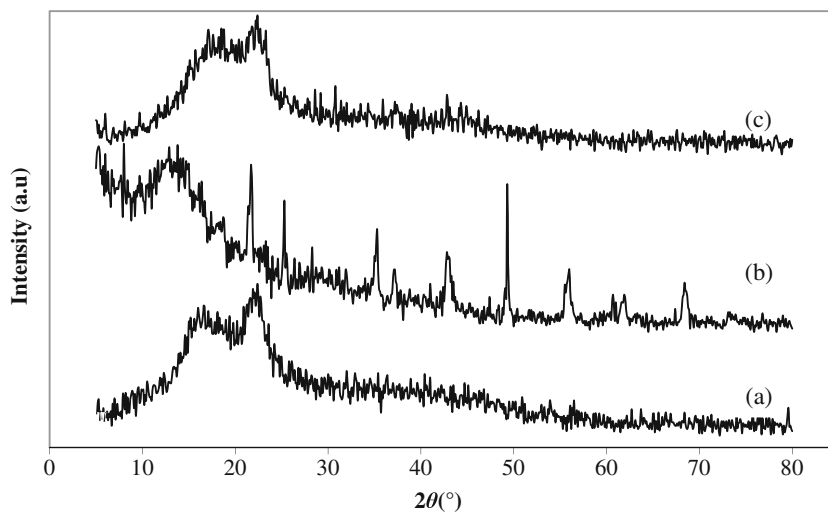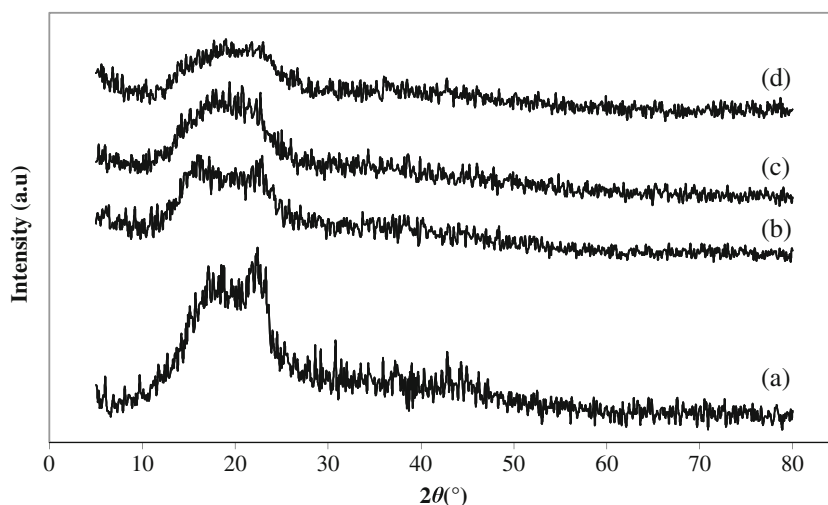**Fig. 5** XRD patterns of *a* pure corn starch, *b* pure $LiPF_6$ and *c* Tf 0

Fig. 6 XRD patterns of *a* Tf 0,
b Tf 3, *c* Tf 5 and *d* Tf 8

backbone, enhancing the segmental mobility of the macro-molecules which confers higher ionic conductivity.

Upon addition of 30 wt.% of BmImTf, T_g of −22 °C is observed. The result is comparable with the ionic liquid-free biopolymer electrolytes because of its deficient plasticizing effect. However, it is also found that plasticizing effect becomes more noticeable with increasing ionic liquid load-ings. It causes the drop in T_g to −24 °C and −29 °C for Tf 5 and Tf 8, respectively, allowing a conclusion that the most ionic conducting character of Tf 8 is ascribed to the stron-gest plasticizing effect which produces the most flexible polymer complex. Therefore, it enhances the mobility of polymer segments significantly and then favors the ionic transportation with a highly flexible polymer backbone.

There is an endothermic peak in the thermogram, which is well-known as the melting peak, T_m. It corresponds to the melting point of BmImTf as no transition is observed for Tf 0 in the temperature regime [18, 19]. Sharp melting peaks are observed for Tf 3 and Tf 5 at 10 °C and 13 °C, respec-tively. In contrast, a weaker peak with smaller peak breadth (or termed as heat of fusion) has been observed for Tf 8 at 15 °C. It reflects the lower crystalline fraction in the polymer

electrolyte compared to Tf 3 and Tf 5. In other words, inclu-sion of 80 wt.% of BmImTf would disorder the ordered arrangement among the macromolecules to the greatest extent. Accordingly, it boosts the flexibility of polymer matrix and ultimately accelerates the ionic movement, increasing the ionic conductivity to a maximum level. Furthermore, the melting temperature of the transition peak increases with the mass ratio of ionic liquid. It is assigned to the formation of self cross-linkage as a result of excessive N–O bonding between BmIm cations and the polymer complex. The higher the ionic liquid quantity, the more cross-linkages would form. Hence, more energy is required to deform the crystalline region into melted form. In conclusion, it exhibits higher melting temper-ature at higher ionic liquid loadings.

Conclusion

Corn starch-based biopolymer electrolytes were prepared by solution casting technique with incorporation of dop-ant salt, $LiPF_6$ and ionic liquid, BmImTf. The highest ionic conductivity of $(6.00\pm0.01) \times 10^{-4}$ S cm^{-1} was achieved

Fig. 7 DSC thermograms of pure corn starch, Tf 0, Tf 3, Tf 5 and Tf 8
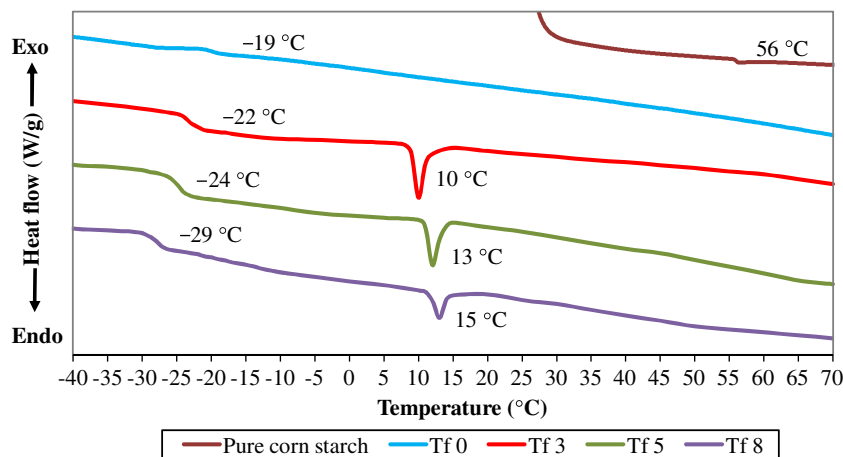
at 80 °C. Temperature dependence–ionic conductivity study verified that the samples exhibit Arrhenius behavior and indicated the ion hopping mechanism in the polymer matrices. Inclusion of ionic liquid helps in demolishing the crystalline phase of the polymer electrolytes, as proven in the XRD analysis. Lower T_g was determined for ionic liquid-based biopolymer electrolytes. This discloses the higher flexibility of polymer electrolytes due to the plasticizing effect of the ionic liquid.

References

1. Shamsipur M, Beigi AAM, Teymouri M, Pourmortazavi SM, Irandoust M (2010) J Mol Liq 157:43–50
2. Liang R, Yang M, Xuan X (2010) Chin J Chem Eng 18:736–741
3. Ramesh S, Liew C-W, Ramesh K (2011) J Non-Cryst Solids 357:2132–2138
4. Xiong H, Tang S, Tang H, Zou P (2008) Carbohydr Polym 71:263–268
5. Pawlicka A, Sabadini AC, Raphael E, Dragunski DC (2008) Mol Cryst Liq Cryst 485:804–816
6. Marcondes RFMS, D'Agostini PS, Ferreira J, Girotto EM, Pawlicka A, Dragunski DC (2010) Solid State Ionics 181:586–591
7. Ma X, Yu J, He K, Wang N (2007) Macromol Mater Eng 292:503–510
8. Magistris A, Mustarelli P, Quartarone E, Tomasi C (2000) Solid State Ionics 136–137:1241–1247
9. Liu J-W, Wang Z-X, Guo H-J, Peng W-J, Zhang Y-H, Hu Q-Y (2010) Trans Nonferrous Met Soc China 20:344–348
10. Zinigrad E, Larush-Asraf L, Gnanaraj JS, Sprecher M, Aurbach D (2005) Thermochim Acta 438:184–191
11. Kim KS, Park SY, Choi S, Lee H (2006) J Power Sources 155:385–390
12. Sankri A, Arhaliass A, Dez I, Gaumont AC, Grohens Y, Lourdin D, Pillin I, R-Sabate A, Leroy E (2010) Carbohydr Polym 82:256–263
13. Aravindan V, Vickraman P, Krishnaraj K (2009) Curr Appl Phys 9:1474–1479
14. Ramesh S, Yin TS, Liew C-W (2011) Effect of dibutyl phthalate as plasticizer on high-molecular weight poly(vinyl chloride)-lithium tetraborate-based solid polymer electrolytes. Ionics. doi:10.1007/s11581-011-0568-9
15. Kumara R, Subramania A, Sundaram NTK, Kumar GV, Baskaran I (2007) J Membr Sci 300:104–110
16. Ramesh S, Liew C-W, Morris E, Durairaj R (2010) Thermochim Acta 511:140–146
17. Baskaran R, Selvasekarapandian S, Kuwata N, Kawamura J, Hattori T (2006) Solid State Ionics 177:2679–2682
18. Huddleston JG, Visser AE, Reichert WM, Willauer HD, Broker GA, Rogers RD (2001) Green Chemistry 3:156–164
19. Xu W, Wang LM, Nieman RA, Angell CA (2003) J Phys Chem B 107:11749–11756